Role of plasma cooling, heating, and memory effects in subpicosecond pulse propagation in semiconductor amplifiers

R. A. Indik
Arizona Center for Mathematical Sciences, Department of Mathematics, University of Arizona, Tucson, Arizona 85721

R. Binder
Optical Sciences Center, University of Arizona, Tucson, Arizona 85721

M. Mlejnek* and J. V. Moloney
Arizona Center for Mathematical Sciences, Department of Mathematics, University of Arizona, Tucson, Arizona 85721

S. Hughes, A. Knorr, and S. W. Koch
Fachbereich Physik und Zentrum für Materialwissenschaften, Phillips-Universität, Renthof 5, D-35032 Marburg, Germany
(Received 11 July 1995)

Based on a microscopic theory of a two-band semiconductor light amplifier, we show that plasma heating, cooling, and ultrafast memory effects all act in concert to produce strong distortion of subpicosecond pulses propagating in semiconductor amplifiers. Plasma heating, spectral hole burning, and carrier density depletion are responsible for saturation of the gain seen by a propagating intense femtosecond pulse in the amplifier. Plasma cooling replenishes the carrier population on the trailing edge of the pulse, leading to pulse broadening as a consequence of gain regeneration. The inclusion of memory effects in the description of dephasing processes goes beyond the usual Markov assumption of constant dephasing rates; it significantly affects the dynamical pulse reshaping processes.

PACS number(s): 42.50.Md, 42.50.Hz, 42.70.Nq, 78.66.−w

I. INTRODUCTION

The propagation of ultrashort light pulses in semiconductor optical amplifiers (SOAs), lasers, and related devices is determined by a wide variety of microscopic processes. Besides the basic stimulated emission processes, which, in direct semiconductors, is determined by the density of states near the Γ point, or, in other words, by the effective masses of electrons and holes, coherent and incoherent many-body effects play a major role. One can roughly categorize these many-body effects as coherent and incoherent, although on a fs time scale these categories might not be strictly separable. Examples of coherent effects are excitonic (Coulombic) enhancement of the gain and absorption spectrum, ultrafast band-gap renormalization due to Coulomb exchange interactions, and nonlinear Coulomb-induced optical field contributions (sometimes called local field effects) [1]. Also, absorption processes leading, in general, to a heating of the charge carrier system can be viewed as coherent effects. Generalized heating mechanisms are two-photon absorption and free-carrier absorption (see, for example [2–8],) and direct band-band absorption in SOAs [9,10].

Examples of incoherent effects are relaxation of carrier distribution functions due to carrier-carrier scattering and thermalization due to carrier-phonon interactions and the dephasing processes of the optical polarization, which results from the incoherent scattering processes. The latter is of greater importance for the description of the linear optical properties, while in the nonlinear regime both dephasing and scattering can influence temporal pulse reshaping considerably. Scattering changes the distribution of charge carriers in momentum space, and, thus, the inversion function in the vicinity of the optical pulse spectrum, which essentially controls the stimulated emission process. In addition, nonlinear phase shifts result from a change in the carrier distribution functions. These processes may yield strong pulse reshaping during the propagation of a pulse through a bulk semiconductor amplifier. Related investigations of ultrashort pulse propagation dynamics in SOAs can be found, for example, in Refs. [4,7,11–14].

The simplest microscopic models of incoherent processes are based on a generalized Markov approximation, where the change of the optical polarization and of the carrier distribution functions at a given time are only related to those functions at the same time. Although these models are often essentially in good agreement with more sophisticated microscopic treatments, certain aspects of the optical linear and nonlinear behavior are sometimes influenced significantly by the use of these models. Especially in the case of dephasing, several investigations have shown that non-Markovian approximations reduce artifacts in the local linear gain-absorption spectra brought about by the dephasing-rate approximation.

The interplay between these processes yields very complicated and interesting nonlinear gain dynamics, both locally and in long-distance propagation. In this paper we will investigate several aspects of these many-body effects and study their influence on propagating subpicosecond pulses. The numerical investigations of the optical processes are based on the semiconductor Bloch equations (SBE) of a two-

*Permanent address: University of Ostrava, Ostrava, Czech Republic.

band semiconductor, which are generalized to include various contributions of carrier correlation effects. In Sec. II we discuss briefly the basic theoretical model for plane-wave pulse propagation in semiconductor media. In Sec. III we discuss a numerical study on the influence of carrier–LO-phonon scattering on subpicosecond pulses and in Sec. IV we include memory (non-Markovian) effects and discuss their influence on the linear and nonlinear gain dynamics.

II. THEORETICAL BASIS

We study a strong femtosecond optical pulse, and assume input plane waves of the form $E(\mathbf{r},t)=\frac{1}{2}[\mathscr{E}(\zeta,\eta)e^{-i\omega_0 t+ik_0 z}+\text{ c.c.}]$ with center frequency ω_0; the pulse is taken to interact with partially inverted GaAs, where optical gain exists in the spectral region between the renormalized band gap and the electron-hole quasichemical potential. The microscopic model known as Maxwell-semiconductor Bloch equations [1,15,16] describes the evolution of the electric field envelope $\mathscr{E}$ in the traveling frame of reference $(\zeta,\eta)=(z,t-zn_b/c)$ (n_b being the background index):

$$\frac{\partial\mathscr{E}(\zeta,\eta)}{\partial\zeta}=\frac{i\mu_0\omega_0^2\Gamma^2}{k_0}\sum_{\mathbf{q}}\ d_{cv}P_{\mathbf{q}}. \tag{1}$$

Confinement in the transverse directions (x and y) is accounted for by the confinement factor Γ, and the momentum-resolved polarization and electron-hole distribution functions, respectively, evolve as

$$\frac{\partial P_{\mathbf{q}}}{\partial t}=-i\Delta_q P_{\mathbf{q}}-i\Omega_q(n_{\mathbf{q}}^e+n_{\mathbf{q}}^h-1)+\left.\frac{\partial P_{\mathbf{q}}}{\partial t}\right|_{\text{scatt}}, \tag{2}$$

$$\frac{\partial n_{\mathbf{q}}^{e/h}}{\partial t}=iP_{\mathbf{q}}^{\star}\Omega_{\mathbf{q}}-iP_{\mathbf{q}}\Omega_{\mathbf{q}}^{\star}+\left.\frac{\partial n_{\mathbf{q}}^{e/h}}{\partial t}\right|_{\text{scatt}}. \tag{3}$$

Here, $\Omega_{\mathbf{q}}=\Omega/2+1/\hbar\Sigma_{\mathbf{q}'}V_{\mathbf{q}-\mathbf{q}'}P_{\mathbf{q}'}$ is the renormalized Rabi frequency, $n_{\mathbf{q}}^{e/h}$ denotes the distribution functions for electrons or holes, and $\Delta_{\mathbf{q}}=\varepsilon_{\mathbf{q}}-\omega_0-(1/\hbar)\Sigma_{\mathbf{q}'}[V_{\mathbf{q}-\mathbf{q}'}(n_{\mathbf{q}'}^e+n_{\mathbf{q}'}^h)+(V_{\mathbf{q}'}-V_{\mathbf{q}'}^0)]$ is the renormalized energy dispersion for a parabolic two-band semiconductor with unrenormalized transition frequency $\varepsilon_{\mathbf{q}}=(1/2m_e+1/2m_h)\hbar q^2+E_g/\hbar$. The Coulomb potential $V_{\mathbf{q}}$ is treated in a quasistatic screening model (except in the case of Fig. 3 discussed below); $V_{\mathbf{q}'}^0$ is the bare potential. The Rabi frequency is $\Omega=d_{cv}\mathscr{E}/\hbar$, where d_{cv} is the dipole matrix element.

These equations contain nonlinear effects such as spectral hole burning, carrier heating due to stimulated emission and direct band-band absorption, and all related nonlinear self-phase modulation effects on a microscopic footing.

Concerning the scattering terms for the carrier distribution functions, our calculations will mainly employ the relaxation rate approximation

$$\left.\frac{\partial n_{\mathbf{q}}^a}{\partial t}\right|_{\text{scatt}}^{cc}=-\gamma_a^{cc}[n_{\mathbf{q}}^a-f_{\mathbf{q}}(\mu^a,T_{\text{pl}})], \tag{4}$$

where f denotes Fermi functions with chemical potentials μ^a and plasma temperature T_{pl} ($a=e,h$). Within this approximation, the plasma temperature has to be computed dynamically because c-c scattering leaves the total kinetic energy of the carrier system unchanged (for details see Appendix B of Ref. [17]).

To justify the relaxation rate approximation for our present studies, we also present calculations based on the quantum Boltzmann equation, where the two-particle Coulomb interaction is dynamically screened within the RPA (random phase approximation) screening function (see, e.g. [17]). The electron-hole Boltzmann equation, for example, can be written as

$$\frac{dn_{\mathbf{q}}^a}{dt}=\Gamma_{\text{in},\mathbf{q}}^a[1-n_{\mathbf{q}}^a]-\Gamma_{\text{out},\mathbf{q}}^a n_{\mathbf{q}}^a, \tag{5}$$

where $\Gamma_{\text{in},\mathbf{q}}^{\mathbf{a}}$ and $\Gamma_{\text{out},\mathbf{q}}^{\mathbf{a}}$ are the usual expressions for in and out scattering. Note, although the relaxation time approximation has been shown to be justified if the semiconductor is sufficiently inverted, for our present studies—in the gain saturation regime—we have shown previously [9] that the nonresonant absorbing states play a very significant role for the propagating pulse, and hence the validity of a **q**-independent scattering rate is not immediately clear.

Within the relaxation rate approximation the incoherent contribution to the polarization function takes the simple form

$$\left.\frac{\partial P_{\mathbf{q}}}{\partial t}\right|_{\text{scatt}}=-\gamma_{q0}P_{\mathbf{q}}, \tag{6}$$

where the total dephasing rate γ_{q0} is one-half times the sum over all individual scattering rates [i.e., summed over all bands and all processes, such as c-c and, if taken into account, c-ph (carrier-phonon) scattering].

Gain saturation in optical amplifiers can be regarded as being a consequence of plasma heating, spectral hole burning, and carrier density depletion. Carrier-carrier scattering ''refills'' the possible spectral holes, but c-c scattering alone does not provide any plasma cooling mechanism. Once the plasma is heated, the carriers are distributed across more momentum states, and fewer of those states are inverted. For subpicosecond pulses, plasma heating is the dominant source of gain saturation. As is nearly always the case with a saturable amplifier, the leading portion of the pulse steepens, and the peak of the pulse actually moves faster than the speed of light in the material. In addition, the refractive index and group velocity dispersion (GVD) are such that the redder frequencies travel faster than the blue. Thus these frequencies end up closer to the leading edge of the pulse, and experience more gain. Consequently, the center of the spectrum of the pulse shifts below the peak of the gain spectrum. Self-phase modulation, as in [27,28] also contributes to this effect, though we believe this effect to be secondary. Finally the GVD due to the background refractive index may contribute to this effect as well. This dispersion has the same sign as the GVD due to the resonant transitions in our model, but we have estimated it using data published in [29] to be significantly smaller, and it has not been included in our calculations.

To address the problem of refilling momentum states that have been depleted by means of stimulated emission, we have to incorporate carrier-phonon scattering into the model. This will be discussed in the following section.

III. PLASMA COOLING INDUCED PULSE RESHAPING

Interaction with the light field, in general, heats the plasma, since the absorption tends to be into high momentum states, creating hot carriers, and the emission removes low momentum carriers. The collision terms, however, should also include terms that describe the cooling of the plasma, since the carriers collide not only with each other, but also with phonons. The optical phonons can take energy from the carriers and couple it to the lattice on the subpicosecond time scale, which is the focus of the present investigation. This process can be only moderately slower than carrier–carrier scattering. We have computed carrier–LO-phonon scattering rates based on the RPA carrier–LO-phonon Boltzmann equation [1].

Relaxation due to carrier-phonon scattering can be taken into account by adding a relaxation rate contribution of the form of Eq. (4), taking the temperature in the Fermi function to be the lattice temperature. The chemical potentials are determined, analogous to the *c*-*c* relaxation rate case, by the condition that the carrier density in each band is not changed by the scattering processes.

On much longer time scales, one must consider that the lattice itself will be heated, and thus the dynamics for T_L may become important (see, for example [18,19]). This much slower thermal process is not relevant to our study.

We have integrated numerically the Maxwell semiconductor Bloch equations given above (similar to Refs. [9,10]) with and without the carrier-cooling contributions (within the relaxation rate approximation). [In this section we concentrate on the effects of cooling within the Lorentzian line-shape approximation, Eq. (6); memory effects will be discussed in the following section.]

The initial conditions are an electron-hole plasma density of $n=2.5\times10^{18}\ \mathrm{cm}^{-3}$ at $T=300$ K. The material parameters used are $m_e=0.067m_0$ (m_0 is the free electron mass), $m_h=0.197m_0$, $n_b=3.56$, and $d_{cv}=5.2e$ Å, and the input pulse parameters are (if not noted otherwise) $\omega_0=E_g+15.2$ meV (at peak gain), $E_g=1.52$ eV, and an initial duration [full width at half maximum (FWHM) in intensity] of 150 fs. The peak amplitude is chosen so that $\hbar\Omega=18.5$ meV at $t=0$. This corresponds to an intensity of $I=(c/8\pi)n_b|\mathscr{E}|^2$ or $I=I_0|\hbar\Omega[\mathrm{meV}]|^2$ with $I_0[\mathrm{GW/cm^2}]=0.01325n_b/(r_{cv}\,[\text{Å}])^2$. In our case $I_0=1.74\ \mathrm{MW/cm^2}$. The confinement factor Γ is chosen to be 0.16. The relaxation rate in the c-c scattering contribution is taken to be $\gamma^{cc}=(60\ \mathrm{fs})^{-1}$ (same for electrons and holes), and, in the solution containing *c*-ph scattering, $\gamma^{e\ -\mathrm{ph}}=(300\ \mathrm{fs})^{-1}$, $\gamma^{h\ -\mathrm{ph}}=(170\ \mathrm{fs})^{-1}$.

As expected, the effect of including the cooling of the plasma is to make the saturation of the gain more difficult. When the plasma cools, carriers move from high momentum states to lower ones and once again become available for stimulated emission. In thin slabs, when the pulses are short enough, there is little effect. To show this, we have computed the intensity at which the net-density change at the front facet of the amplifier (i.e., density after the pulse minus initial density) is zero (this effect has been discussed in Ref. [9]). Table I shows how the peak intensity (presented in terms of the corresponding Rabi frequency $\hbar\Omega_s$) at which the gain is saturated varies with pulse length with and without cooling. Obviously, the effect of cooling in this regime of strong gain saturation is rather small if only the front facet is being considered and if the pulse is shorter than the *c*-ph relaxation time. For pulses longer than this time the effect is, as expected, significant: it takes considerably higher intensities to obtain zero net-density change if the cooling, which refills the resonant gain states, is present.

TABLE I. $\hbar\Omega_s$ with and without cooling as a function of the pulse length.

Pulse length (FWHM)	$\hbar\Omega_s$ (no cooling)	$\hbar\Omega_s$ (with cooling)
100 fs	21.89 meV	22.85 meV
200 fs	16.39 meV	18.81 meV
400 fs	12.03 meV	16.49 meV
800 fs	8.67 meV	15.78 meV
1600 fs	6.18 meV	17.78 meV

For the short 150-fs pulse, which is even stronger than the above-discussed zero-net-density-change pulse, we show in Fig. 1 the density response in the front facet of the SOA as it is affected by the cooling—compare the solid and dotted lines. Clearly, the cooling-induced stimulated emission does not influence the density in a significant way. The corresponding temporal behavior of the generalized plasma temperature T_{pl} for the three line-shape models is shown in Fig. 2. (The generalized plasma temperature can be extracted from the kinetic energy of the carriers.) As expected, emission of LO phonons reduces the temperature after the pulse has passed.

To investigate the validity of the carrier momentum independent scattering rate restriction, we also present calculations employing a direct numerical solution of the carrier-

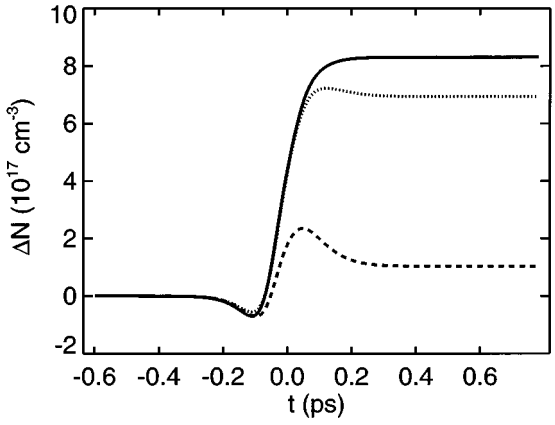

FIG. 1. Comparison of density response in the front facet of the amplifier for different models. Solid line: Lorentzian line-shape model, no cooling. Dotted line: Lorentzian line-shape model, cooling included. Dashed line: memory model (parameters according to Fig. 6), cooling included. The initial condiditions, material parameters, and pulse parameters are given in the text. The peak amplitude of the pulse is 38 meV.

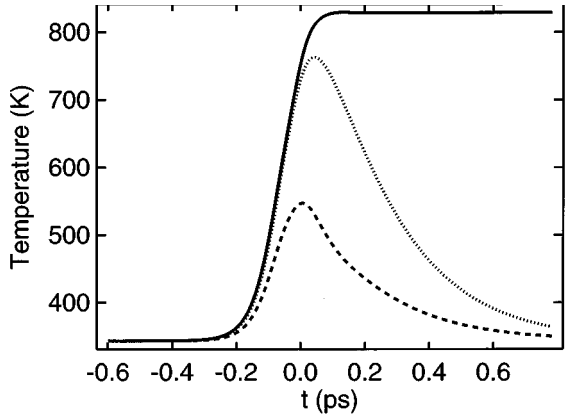

FIG. 2. Generalized plasma temperature, extracted from the kinetic energy of the nonequilibrium distribution functions, corresponding to Fig. 1.

carrier Boltzmann equation. Figure 3 shows the density response in the front facet of the SOA for increasing input intensities that incorporate the **q**-dependent scattering rates, which further depend on time and density. These calculations show clearly that gain is saturated and there is a net absorption as in the solid line of Fig. 1. Even though the calculated dephasing times are larger around the nonresonant states than in the excitation region, the linewidths are still sufficient to allow absorption from the nonresonant states to dominate for high input fields. This model does not include interactions with optical phonons (cooling), or memory effects, and so should be compared to the simplest relaxation rate approximation as in Eq. (4). The rest of the calculations presented in this paper will follow within the relaxation time approximation, without any loss of generality.

Figure 4 shows the time evolution of the intensity of the pulse after various propagation distances; for longer propagation lengths, we see that cooling has a dramatic effect even for pulses that are initially very short. Where previously the gain was depleted by the leading portion of the pulse, we

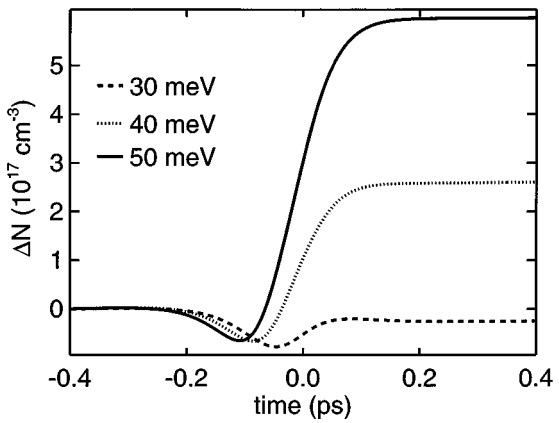

FIG. 3. The time evolution of the density for increasing input intensities, whereby the relaxation rates are calculated using the full RPA dynamical screening Boltzmann equations. The results shown do not include cooling or memory effects. For increasing Rabi frequency (up to $\hbar\Omega = 50$ meV), saturation of the gain and increasing carrier density are seen clearly.

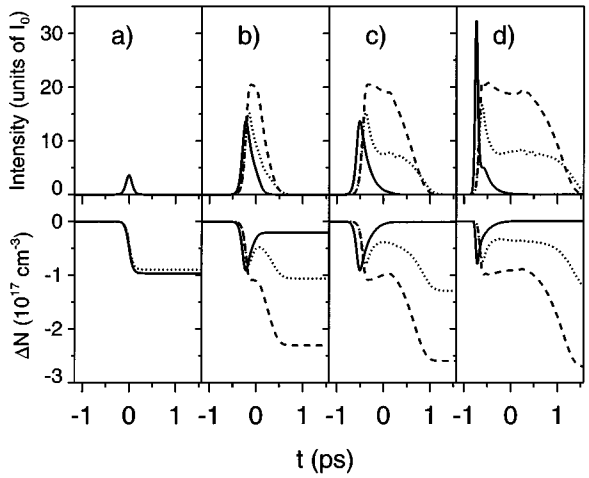

FIG. 4. The upper trace shows intensity in units of I_0 vs time for various propagation distances (in units of μm): 0, 250, 500, and 750 (from left to right) (line styles same as in Fig. 2). The lower trace shows density change $\Delta N(t) = n(t) - n(t = -\infty)$.

now see that the cooled carriers produce additional gain on the trailing portion of the pulse. The leading edge of the pulse is not greatly changed (at least qualitatively), but now the vast bulk of the energy in the pulse is on the trailing portion. To take advantage of the very sharp leading portion of the pulse, it would have to be separated from its much larger tail.

IV. MEMORY EFFECTS

In the preceding sections all scattering contributions to the equations of the optical polarization function and carrier distribution functions were based on the so-called Markov approximation: the time evolution of P and n at a given time t depends only on the values of P and n at the same time. It is well known, however, that the microscopic description of the correlation contributions contain memory effects; i.e., they contain time integrations of P and n over all times $t' \leqslant t$:

$$\gamma_{q0} P_{\mathbf{q}}(t) \rightarrow \int_{-\infty}^{t} dt' \, \gamma_{q0}(t - t') P_{\mathbf{q}}(t'). \tag{7}$$

Within the Markov approximation, these memory effects can be neglected if the memory depth (the time interval in t' in which the integrand is nonzero) approaches zero. A typical value of the memory depth is the relaxation or scattering time, which is dominated by carrier-carrier or carrier-phonon collisions. Although this time is often very short (in our example it is 60 fs; see above), the complete neglect of memory effects can result, in certain situations, in significant modifications of the computed behavior of the polarization and/or distribution functions.

One of the best known examples of optical phenomena influenced by non-Markovian effects occurs in the theory of the linear optical response of a noninverted semiconductor, or, more specifically, in the theory of the spectral line shape of bound exciton resonances. Within the Markov approximation the line shape is Lorentzian, with spectral width γ. But

even in stationary (cw) absorption measurements the observed absorption line shape of the lowest exciton resonance is, in its tail, exponential rather than Lorentzian (Urbach tail). In the noninverted semiconductor the microscopic processes responsible for the specific line shape are mainly electron–LO-phonon interactions and exciton trapping (see, for example [20–22],). Further recent studies of linear and nonlinear optical effects in semiconductors influenced by non-Markovian behavior of the photoexcited charge carriers include Refs. [23–26,30].

For our present investigation of semiconductor amplifiers, studies of non-Markovian correlation effects in electron-hole plasmas are directly relevant. As we will show in the following, these effects are particularly important in the gain saturation regime. Inclusion of the microscopic expressions for non-Lorentzian line shapes along the lines of Refs. [31–33] results in a significant improvement of the theoretical analysis of ultrafast light amplification and absorption. It allows for a correct description of off-resonant light coupling (i.e., coherent interaction with band-band transitions not in resonance with the light field); this eliminates the well-known artificial absorption below the gain region that results from the use of Lorentzian line shapes [1,31]. The main restriction of the theories referenced above is the limitation to the linear response regime, in which the carrier distribution functions are time independent. Similar to the Markovian relaxation rates, it has been found that non-Markovian scattering in inverted semiconductors is dominated by carrier-carrier scattering, especially the hole-hole scattering contributions [31]. In addition to incoherent carrier-carrier and carrier–LO-phonon scattering, a line-shape analysis of semiconductor gain spectra has revealed the possibility of plasmon-phonon side bands in the low-energy tail of the gain spectrum [34]. However, in the following we will restrict ourselves to incoherent scattering processes.

For implementation of the existing line shape and non-Lorentzian dephasing theories into numerical algorithms of ultrashort light pulse propagation, it is imperative to have a simple parametrization of the complicated line-shape expressions of Refs. [31–33]. The goal of this section is to present and discuss various models that can be used to simulate non-Lorentzian line shapes and to discuss in detail their influence on ultrafast gain saturation dynamics. In particular, we propose a specific model (the so-called ''two-pole model'') that allows for a computationally highly optimized simulation of non-Lorentzian line-shape effects. One may compare the two-pole model to already existing models, such as the ''sech'' model [1]. The reason that we formally separate renormalization effects [i.e., the real self-energy contribution to Eq. (2)] from incoherent dephasing effects is related to the fact that the relative importance of self-energy versus dephasing terms depends on the specific approximation scheme being used. All dephasing processes are, theoretically, contributions beyond the quasi-statically screened Hartree-Fock (HF) approximation, which yields only the real self-energy and field renormalization terms in the semiconductor Bloch equations. The correlation contributions obtained from a theory that goes beyond the HF approximation contains, in addition to dephasing and relaxation, energy renormalization terms. We believe that for the study of gain saturation only the dephasing-relaxation terms are important, while the additional self-energy terms can be neglected. However, it is pointed out in Ref. [31] that one consequence of the self-energy renormalization beyond the HF regime is an asymmetry of the line-shape function, which we include in our model.

As an explicit example for the non-Markovian dephasing function [see Eq. (7)], we use

$$\gamma_{\mathbf{q}}(t)=\gamma_{1q0}\gamma_{2q0}e^{-(\gamma_{1q0}+\gamma_{2q0}+i\omega_{\mathbf{q}})t}. \tag{8}$$

The corresponding non-Lorentzian line shapes will have a quartic falloff with detuning, which is desired because it essentially removes the spurious below-band-gap absorption.

We call (8) a two-pole model, as in Fourier space the response function corresponding to the diagonal linear terms in the $P_{\mathbf{q}}$ can be written as a rational function with two poles in the complex upper half plane. One very convenient feature of such a form is that it is easily converted back into a system of coupled ordinary differential equations. We replace Eq. (6) with a pair of equations:

$$\left.\frac{\partial P_{\mathbf{q}}}{\partial t}\right|_{\text{scatt}}=-\gamma_{1q0}S_{\mathbf{q}0}, \tag{9}$$

$$\frac{\partial S_{\mathbf{q}}}{\partial t}=(-\gamma_{1q0}-\gamma_{2q0}+i\omega_{\mathbf{q}})S_{\mathbf{q}}+\gamma_{2q0}P_{\mathbf{q}}. \tag{10}$$

Assuming a two-pole form for the response is equivalent to replacing the Markovian assumption that leads to the Lorentzian line shape with a two-stage Markovian assumption.

Our preferred set of parameters is chosen to fit the two-pole line-shape model to the line shape obtained by Yamanishi and Lee [31]. This is shown in Fig. 5. [Concerning the overall width, we choose $(60\ \text{fs})^{-1}$ in our calculations instead of $(100\ \text{fs})^{-1}$ calculated by Yamanishi and Lee. Fitting the two-pole model to the sech line-shape model discussed in Ref. [1], we find a memory time $(\gamma_{2q0})^{-1}$ of 20 fs, which is much closer to the overall relaxation time of 60 fs for *c-c* scattering.]

Although only present on a very short time scale, memory effects can have a pronounced effect on, for example, linear gain spectra. In Fig. 6 we compare the three models (Lorentzian, two-pole fitted to Ref. [31], and two-pole fitted to Ref. [1]). Regardless of the exact value of the memory time (3 or 20 fs) the spurious absorption below the band gap is reduced drastically within the two-pole model. Concerning the numerical value of the gain throughout the gain region, we see that even a memory time as short as 3 fs results in a strong gain increase when compared to the Lorentzian results, indicating the decreased role of high-momentum band-band transition (i.e., absorptive transitions) for the optical gain. Whereas in Fig. 6 we compare spectra for the same density, which have different peak gain values within the different models, in Fig. 7 we adjust the density for each model to yield the same peak gain. The following study of line-shape effects will be based on this latter comparison; i.e., the same peak gain value underlies the results for the various line-shape models.

In order to study the effects of non-Lorentzian line shapes on nonlinear pulse propagation, we show in Figs. 1 and 4 the corresponding results with memory effects included. The

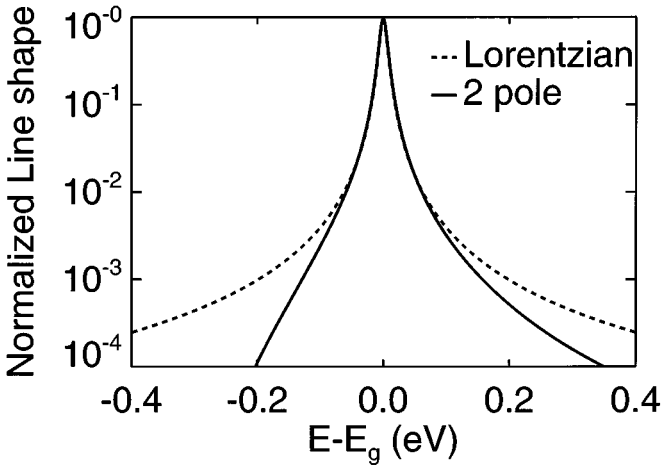

FIG. 5. Logarithmic plot of line-shape function used to model memory effects (solid line) and corresponding Lorentzian line-shape function (dashed line) with $\gamma^{cc}=(60\ \mathrm{fs})^{-1}$. The non-Lorentzian line shape is obtained using the two-pole model discussed in the text by fitting it to the line shape based on a microscopic theory of Ref. [31].

memory model used is the two-pole approximation with 3-fs memory time. From Fig. 1 we see how the absorption into high-momentum states, which is responsible for the net-density increase, is reduced by memory effects. This reduction of the net density increase is accompanied by an enhanced transient density increase, which can be ascribed to adiabatic following contributions (i.e., the occupation of high-momentum states roughly follows the intensity, not the time integral of the intensity).

For long-distance propagation, Fig. 4 shows that memory effects lead to a strong enhancement of the trailing portion of the pulse, whereas their influence on the leading edge of the pulse is much less significant. In general, the amplification of the pulse, and, in particular, the trailing portion, is stronger if gain saturation is inhibited and carrier heating is reduced.

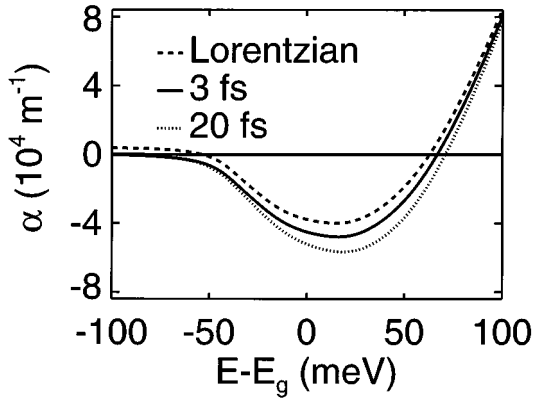

FIG. 6. Linear gain spectra comparing the Lorentzian line-shape model to the non-Lorentzian line-shape models evaluated in the two-pole approximation with parameters adjusted to fit the line shape of Yamanishi and Lee [31] (memory time of 3 fs) and the sech line shape discussed on p. 94 in Ref. [1] (memory time of 20 fs). The density is $n=2.5\times10^{18}\ \mathrm{cm}^{-3}$ at $T=300$ K.

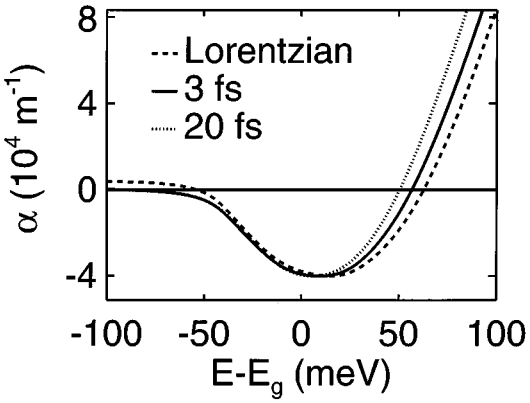

FIG. 7. Same as Fig. 6, but the density is adjusted so that the peak gain has the same value for the different models. Solid line: $n=2.265\times10^{18}\ \mathrm{cm}^{-3}$; dotted line: $n=2.020\times10^{18}\ \mathrm{cm}^{-3}$; dashed line: $n=2.500\times10^{18}\ \mathrm{cm}^{-3}$.

The inclusion of memory effects inhibits gain saturation and decreases carrier heating, because carrier heating results mainly from absorption into noninverted momentum states (see Fig. 2). Memory effects clearly reduce the transient heating.

V. SUMMARY

Our studies of femtosecond pulse propagation in bulk semiconductor amplifiers have revealed a subtle and complex interplay between various physical mechanisms that can be ascribed to coherent and incoherent many-body effects. In particular, we have systematically studied the role of carrier-carrier scattering, carrier-phonon scattering, and memory effects on femtosecond pulse propagation. Plasma cooling and memory effects are shown to lead to a pronounced amplification of the trailing portion of the pulse and, hence, severe pulse distortion. Additional effects, such as two-photon absorption and free-carrier absorption, are beyond the scope of this paper, since they pose a formidable task concerning the study of pulse propagation based on fully microscopic semiconductor models. For a detailed experiment-theory comparison, however, it would be desirable to include such effects. The purpose of the present paper is to study the role of certain microscopic processes on nonlinear gain dynamics of semiconductor optical amplifiers and the long-distance propagation of sub-picosecond pulses.

ACKNOWLEDGMENTS

Support for this work from the Arizona Center for Mathematical Sciences under Grant No. AFOSR F49620-94-1-00144DEF is acknowledged, with partial support from the Optical Circuitry Cooperative, University of Arizona. J.V.M. and S.W.K. acknowledge travel support from NATO and partial support through the Commission of the European Communities. S.H. thanks the the Commission of the European Communities for a financial support. Computing support was provided by the DOD High Performance computing center at Maui.

[1] W. W. Chow, S. W. Koch, and M. S. III, *Semiconductor-Laser Physics* (Springer, Berlin, 1994).
[2] M. P. Kesler and E. P. Ippen, Appl. Phys. Lett. **51**, 1765 (1987).
[3] K. L. Hall, Y. Lai, E. P. Ippen, G. Eisenstein, and U. Koren, Appl. Phys. Lett. **57**, 2888 (1990).
[4] M. Willatzen, A. Uskov, J. Mørk, H. Olssen, B. Tromborg, and A. P. Jauho, IEEE Photonics Techn. Lett. **3**, 606 (1991).
[5] K. L. Hall, G. Lenz, E. P. Ippen, U. Koren, and G. Raybon, Appl. Phys. Lett. **61**, 2512 (1992).
[6] J. Zhou, N. Park, J. W. Dawson, and K. J. Vahala, Appl. Phys. Lett. **63**, 1179 (1993).
[7] C.-K. Sun, H. K. Choi, C. A. Wang, and J. G. Fujimoto, Appl. Phys. Lett. **62**, 747 (1993).
[8] J. R. Karin, A. V. Uskov, R. Nagarajan, J. E. Bowers, and J. Mørk, Appl. Phys. Lett. **65**, 2708 (1994).
[9] A. Knorr, R. Binder, E. Wright, and S. Koch, Opt. Lett. **18**, 1538 (1993).
[10] R. Indik, A. Knorr, R. Binder, J. Moloney, and S. W. Koch, Opt. Lett. **19**, 966 (1994).
[11] P. Delfyett, Y. Silberberg, and G. Alphonse, Appl. Phys. Lett. **59**, 10 (1991).
[12] J. Mark and J. Mørk, Appl. Phys. Lett. **61**, 2281 (1992).
[13] A. Dienes, J. Heritage, M. Hong, and Y. Chang, Opt. Lett. **17**, 1602 (1992).
[14] A. Uskov, J. Mørk, and J. Mark, IEEE Photonics Techn. Lett. **4**, 443 (1992).
[15] W. Schäfer and K. Henneberger, Phys. Status Solidi B **159**, 59 (1990).
[16] A. Knorr, R. Binder, M. Lindberg, and S. W. Koch, Phys. Rev. A **46**, 7179 (1992).
[17] R. Binder, D. Scott, A. E. Paul, M. Lindberg, K. Henneberger, and S. W. Koch, Phys. Rev. B **45**, 1107 (1992).
[18] C. Z. Ning, R. Indik, and J. V. Moloney, J. Opt. Soc. Am. B (to be published).
[19] C. Z. Ning and J. V. Moloney, Appl. Phys. Lett. **66**, 559 (1995).
[20] J. Liebler, S. Schmitt-Rink, and H. Haug, J. Lumin. **34**, 1 (1985).
[21] H. Haug, J. Liebler, R. Leonelli, A. Manar, and J. Grun, Phys. Rev. B **38**, 10 903 (1988).
[22] R. Zimmermann, Phys. Status Solidi B **159**, 317 (1990).
[23] W. Vogel, D.-G. Welsch, and B. Wilhelmi, Phys. Rev. A **37**, 3825 (1988).
[24] A. V. Kuznetsov, Phys. Rev. B **44**, 8721 (1991).
[25] D. K. Ferry, A. M. Kriman, H. Hida, and S. Yamaguchi, Phys. Rev. Lett. **67**, 633 (1991).
[26] M. Hartmann and W. Schäfer, Phys. Status Solidi (B) **173**, 165 (1992).
[27] G. P. Agrawal, J. Opt. Soc. Am B, **5**, 147 (1988).
[28] P. Heist, W. Rudolph, and V. Petrov, Appl. Phys. B **49**, 113 (1989).
[29] *Semiconductors: Group IV Elements and III-V Compounds*, edited by O. Madelung, Landolt-Börnstein, New Series, Group III, Vol. 17, Pt. a (Springer-Verlag, Berlin, 1991), Fig. 12 on p. 108.
[30] J. Schilp, T. Kuhn, and G. Mahler, Phys. Rev. B **50**, 5435 (1994).
[31] M. Yamanishi and Y. Lee, IEEE J. Quantum Electron. **14**, 367 (1987).
[32] T. Ohtoshi and M. Yamanishi, IEEE J. Quantum Electron. **27**, 46 (1991).
[33] M. Asada, in *Quantum Well Lasers*, edited by P. Zory (Academic, New York, 1993), pp. 97–130.
[34] J. F. Müller and H. Haug, J. Lumin. **37**, 97 (1987).